Determination of vertical derivative of gravity anomalous by upward continuation and Taylor series transform methods: application to the Southwest sub-basin of the East Vietnam Sea

Nguyen Nhu Trung[1,2,*], Tran Van Kha[1], Bui Van Nam[1,2]

[1]Institute of Marine Geology and Geophysics, VAST, Vietnam
[2]Graduate University of Science and Technology, VAST, Vietnam
[*]E-mail: nntrung@imgg.vast.vn

ABSTRACT

The vertical derivative of the gravity anomaly has a vital role in the methods of geological structure research such as determining fault systems and the location of the field sources. In addition, the vertical derivative is also used to calculate the downward continuation and further clarify the image of the seabed topography. However, determining the vertical derivative according to the traditional Fast Fourier Transform (FFT) method is often unstable and has low accuracy in high-order derivatives for high noise actual data. In this article, we introduce a new calculation method to determine the vertical derivative of gravity anomaly giving higher stable and accurate than traditional methods. The method is verified on synthetic model data and actual data of the Southwest sub-basin of the East Vietnam Sea.

Keywords: Gravity anomaly, vertical derivative, Taylor series, fast Fourier transform.

INTRODUCTION

Calculating the vertical derivative of gravity anomaly is an essential method in gravimetric data processing methods to determine the boundary of geological structure or fault system [1–5]. In addition, the vertical derivative is also used in calculating the downward continuation [6–12] to increase the accuracy when determining the topography of boundary surfaces such as sedimentary foundations and seabed topography [13, 14]. It is easy to see that the vertical derivative dramatically affects the accuracy of the above calculation methods. In previous studies, the authors mainly used the vertical derivative through the frequency domain, such as fast Fourier transform (FFT), Hilbert transform [15, 16], or the method of Laplace equation [17]. However, Kha and Trung [12] published a new technique using the the upward continuation and Taylor series expansion methods (UCT) to calculate the vertical derivative, and showed that the calculation of the vertical derivative through the frequency domain is unstable when the data have noises, especially in case of higher-order vertical derivatives, which can affect the results of determining the structural boundary as well as the stability in the downward continuation problem. This UCT method has increased the accuracy and stability of the calculation of the higher order vertical derivatives than previous traditional methods such as FFT, Hilbert, or Laplace methods. Recently, some authors have also been used the UCT method in calculating

gravity tensors [18–20], the vertical derivative in determining the structural boundaries of the Witwatersrand basin, South Africa [3]. Trung et al., (2020) [14] used the UCT method to calculate the downward continuation of the Bouguer anomaly data to the near seabed, then reverted this downward continuation gravity anomaly data to determine the sediment basement. The obtained results have higher resolution and reliability than the conventional calculation method.

To see the important application meaning of calculating the vertical derivative in the analysis of gravity data, in this article, we introduce the method of calculating the first and second vertical derivatives of the gravity anomaly according to the UCT method [12]. The results of applying the UCT method to calculate the vertical derivative of gravity anomalies have been verified on synthetic model data and actual data in the Central Basin of the East Vietnam Sea, giving results with high accuracy and stability than previous traditional methods, especially in the case of high random noise data.

THEORETICAL BASIS OF THE METHOD

Assuming $f(x, y, z)$ is a potential field measured at an observation plane of height z, in the Decartes coordinate system, the z-axis positive direction is downward. The potential field at height $(z - \Delta h)$ is $f(x, y, z - \Delta h)$ which can be represented by Taylor series as follows [7, 17]:

$$f\left(x,y,z-\Delta h\right) = f\left(x,z\right) - \Delta h f'\left(x,y,z\right) + \frac{\Delta h^2}{2!}f'' + ... + \frac{\left(-\Delta h\right)^n}{n!}f^n\left(x,y,z\right) \qquad (1)$$

where: $(f'(x, y, z), f''(x, y, z),…, f^n(x, y, z))$ are the vertical derivatives in order of 1, 2,…, n. In this study, we do not determine these vertical derivative values according to the traditional fast Fuorier transform (FFT) method, but determine them through the gravity anomaly at

the different upward continuation level ($f(x, y, z - \Delta h), f(x, y, z - 2\Delta h),…, f(x, y, z - n\Delta h)$).

We consider equation (1) with a Taylor series expansion of $n = 1, 2,…, N$ and Δh is positive and small enough, then we have the following system of equations:

$$
\begin{cases}
f(x,y,z-\Delta h) = f(x,y,z) - \Delta h f'(x,y,z) + \dfrac{(-\Delta h)^2}{2!} f''(x,y,z) + \ldots + \dfrac{(-\Delta h)^n}{n!} f^n(x,y,z) \\[2mm]
f(x,y,z-2\Delta h) = f(x,y,z) - 2\Delta h f'(x,y,z) + \dfrac{(-2\Delta h)^2}{2!} f''(x,y,z) + \ldots + \dfrac{(-2\Delta h)^n}{n!} f^n(x,y,z) \quad (2) \\[2mm]
f(x,y,z-n\Delta h) = f(x,y,z) - n\Delta h f'(x,y,z) + \dfrac{(-n\Delta h)^2}{2!} f''(x,y,z) + \ldots + \dfrac{(-n\Delta h)^n}{n!} f^n(x,y,z)
\end{cases}
$$

The equations (2) can be written in the form of matrix equation (3) as follows:

$$
\begin{pmatrix}
-\Delta h & \dfrac{(-\Delta h)^2}{2!} \cdots & \dfrac{(-\Delta h)^n}{n!} \\[3mm]
-2\Delta h & \dfrac{(-2\Delta h)^2}{2!} \cdots & \dfrac{(-2\Delta h)^n}{n!} \\
& \vdots & \\
-n\Delta h & \dfrac{(-n\Delta h)^2}{2!} & \dfrac{(-n\Delta h)^n}{n!}
\end{pmatrix}
\begin{pmatrix}
f'(x,y,z) \\[1mm]
f''(x,y,z) \\
\vdots \\
f^n(x,y,z)
\end{pmatrix}
=
\begin{pmatrix}
f(x,y,z-\Delta h) - f(x,y,z) \\[1mm]
f(x,y,z-2\Delta h) - f(x,y,z) \\
\vdots \\
f(x,y,z-n\Delta h) - f(x,y,z)
\end{pmatrix}
\quad (3)
$$

Solve the linear matrix equation (3) with the unknowns being the derivatives of order $n = 1, 2,\ldots, N$ ($f'(x, y, z)$, $f''(x, y, z),\ldots,$ $f^n(x, y, z)$).

For $n = 8$, solving equation (3) we get the vertical derivatives from the 1st to 8th order. Here is the definite formula for the vertical derivatives of the 1st, 2nd and 3rd order:

$$
\begin{aligned}
f'(x,y,z) = & \frac{2283 f(x,y,z) - 6720 f(x,y,z-\Delta h) + 11760 f(x,y,z-2\Delta h) - 15680 f(x,y,z-3\Delta h)}{840\Delta h} \\[2mm]
& + \frac{14700 f(x,y,z-4\Delta h) - 9408 f(x,y,z-5\Delta h) + 3920 f(x,y,z-6\Delta h) - 960 f(x,y,z-7\Delta h) + 105 f(x,y,z-8\Delta h)}{840\Delta h}
\end{aligned}
\quad (4)
$$

$$
\begin{aligned}
f''(x,y,z) = & \frac{29531 f(x,y,z) - 138528 f(x,y,z-\Delta h) + 312984 f(x,y,z-2\Delta h) - 448672 f(x,y,z-3\Delta h)}{5040\Delta h^2} \\[2mm]
& + \frac{435330 f(x,y,z-4\Delta h) - 284256 f(x,y,z-5\Delta h) + 120008 f(x,y,z-6\Delta h) - 29664 f(x,y,z-7\Delta h)}{5040\Delta h^2} \\[2mm]
& + \frac{3267 f(x,y,z-8\Delta h)}{5040\Delta h^2}
\end{aligned}
\quad (5)
$$

$$
\begin{aligned}
f'''(x,y,z) = & \frac{2403 f(x,y,z) - 13960 f(x,y,z-\Delta h) + 36706 f(x,y,z-2\Delta h) - 57384 f(x,y,z-3\Delta h)}{240\Delta h^3} \\[2mm]
& + \frac{58280 f(x,y,z-4\Delta h) - 39128 f(x,y,z-5\Delta h) + 16830 f(x,y,z-6\Delta h) - 4216 f(x,y,z-7\Delta h)}{240\Delta h^3} \\[2mm]
& + \frac{469 f(x,y,z-8\Delta h)}{240\Delta h^3}
\end{aligned}
\quad (6)
$$

The 1st, 2nd, and 3rd vertical derivative in the fomulas (7), (8), and (9) are defined from the gravity anomalies upward continued at the elevation $\Delta h, 2\Delta h,\ldots, 8\Delta h$. Calculation results using these formulas give us a more stable and accurate vertical derivative value than other

conventional calculation methods, especially in the case of noisy data [12].

APPLY ON SYNTHETIC MODEL

The theoretical model investigated in this study is a rectangular prism with physical parameters, as shown in Table 1. Gravity anomalies on the obseved surface of the rectangular prism are shown in Figure 1a. The

first, second, and third order vertical derivatives of the gravity anomaly of the rectangular prism are calculated by equations (4), (5), and (6) for both correct gravity anomaly data (without random noise) and plus 5% random noise. The results of calculating the vertical derivative by formulas (4), (5) and (6) are compared with the result of calculating the vertical derivative by the traditional FFT method.

Table 1. Physical parameters of the prism model

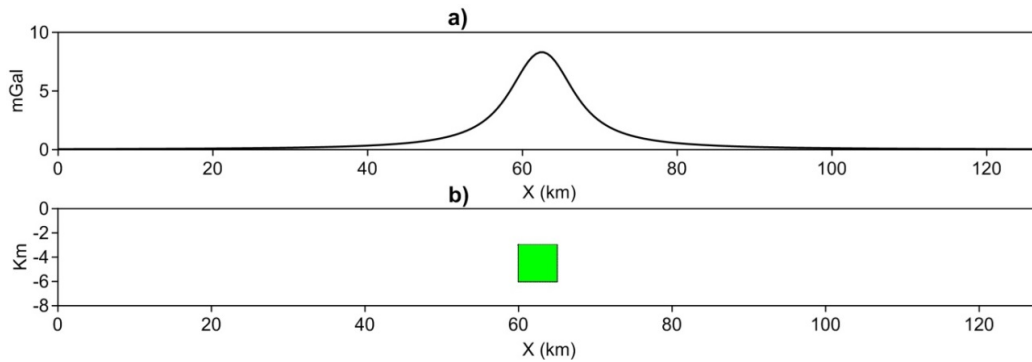| X_1 (km)	X_2 (km)	D_x (km)	Z_1 (km)	Z_2 (km)	Mật độ dư (g/cm^3)
60	65	0.5	3	6	0.2

Figure 1. a) Gravity anomaly of rectangular prisms; b) Rectangular prism model
with physical parameters in Table 1

The calculation results of the first, second, and third order vertical derivatives in Figure 2 show that in the case of data without noise (exact data), the difference between the vertical derivative is calculated by the FFT method and the UCT method is a minimal error and almost the same (Table 2 and

Figure 2). The vertical derivative values have minor errors compared with the theoretical values in all three cases of first, second, and third derivatives (Table 2). Thus, with correct data, the vertical derivatives are calculated by the FFT method, and the UCT method does not see the difference.

Table 2. Root mean square error (RMSE) of the first, second and third order vertical derivatives
are caluclated by FFT and UCT methods in the case of the correct gravity anomaly

Root mean square error	The 1st vertical derivative (mGal)	The 2nd vertical derivative (mGal)	The 3rd vertical derivative (mGal)
FFT method	0.00267	0.00086	0.00154
UCT method	0.00267	0.00086	0.00144

When the gravity anomaly is added 5% random noise, the vertical derivative calculated by the UCT and the FFT methods are very different (Figure 3). The vertical derivative calculated by the FFT method gives very poor results. The vertical

derivative value is noisy and unstable: The first order vertical derivative (red line in Figure 3a) appears relatively large sawtooth pulses at the high anomalous amplitude region. The 2nd and 3rd order derivatives (red lines in Figures 3b and 3c) are instability, the

vertical derivative value is strongly perturbed, and the amplitude is completely different from its true value (amplitude is larger 10 times for the second-order derivative and 100 times for the third-order derivative). The vertical derivative calculated by the UCT method gives very good results in the first-order vertical derivative (Figure 3a), and even with the second-order vertical derivative, the value is consistent with the theoretical value (3b). For the third order vertical derivative (Figure 3c), although there is a discrepancy between the theoretical and calculated results, the shape of the vertical derivative graph is quite consistent with the theoretical derivative.
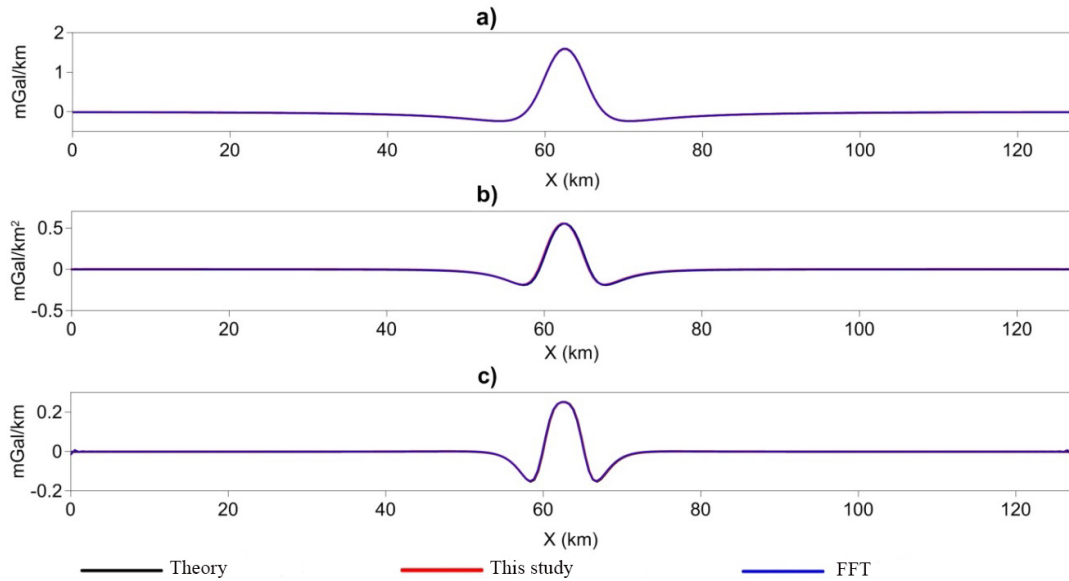

Figure 2. The vertical derivative of gravity anomaly of the rectangular prism calculated by the FFT method and the UCT method almost coincides with the theoretical value; a) the first order vertical derivative; b) the 2nd order vertical derivative; c) the 3rd order vertical derivative
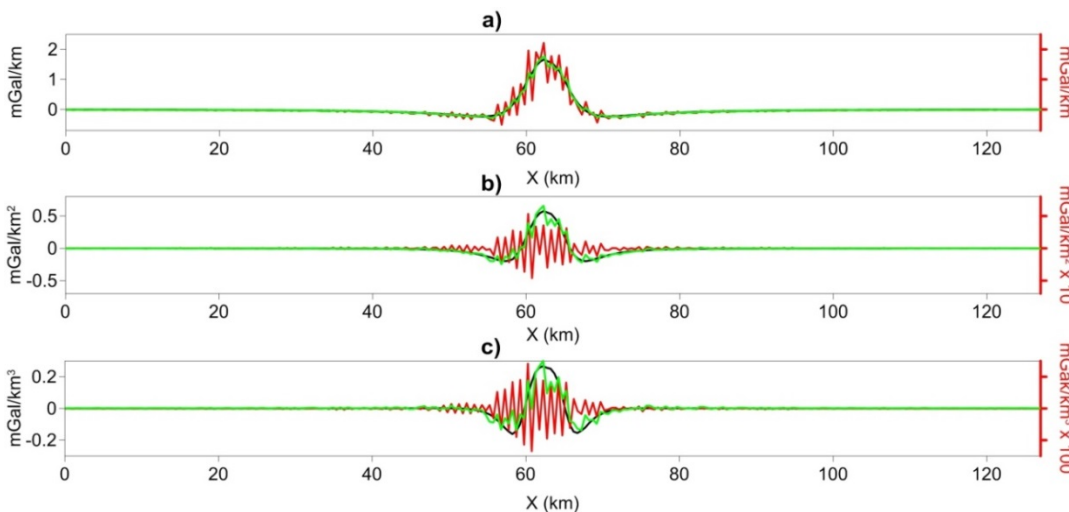

Figure 3. Vertical derivative of gravity anomaly of a prism (Figure 1) when the gravity anomaly is added 5% random noise; a) the 1st order vertical derivative; b) the 2nd order vertical derivative; c) the 3rd order vertical derivative

Thus, it can be seen that, in the case of measured data with random noise, the calculation of the vertical derivative by the method proposed by Kha and Trung (2020) [12] gives very high accurate and stable results while the results calculated by the FFT method have low accuracy and unstable results, especially in the case of second and third order derivatives.

VERTICAL DERIVATIVE OF GRAVITY ANOMALY IN THE SOUTHWEST OF THE CENTRAL BASIN, EAST VIETNAM SEA

The study area is located in the southwest of the Central Basin of the East Vietnam Sea (Figure 4), including the area of the Southwest sub-basin in the center, a part of the Hoang Sa islands in the North and a part of the Truong Sa islands in the South (Figure 4a). Figure 4b is the Bouguer gravity anomaly calculated from the free-air satellite gravity anomaly data with 1' × 1' resolution (https://topex.ucsd.edu/cgi-bin/get_data.cgi), V29.1 [22] and bathymetry data from GEBCO source with 15" × 15" resolution. (https://www.gebco.net/data_and_products/gridded_bathymetry_data/). The results of calculating the first-order vertical derivative by the UTC method (Figure 5a) have stable values, except for some areas Northeast of the Southwest sub-basin. The first order vertical derivative map has sharp positive and negative anomalies, clearly reflecting the geological structure system in the study area, such as spreading ridge axis, continental - oceanic crust boundary, NE-SW fault system, and sub-meridian, sub-latitude faults (Figure 4a and Figure 5a). The first order vertical derivative map calculated by the FFT method gives much worse results: in the Southwest sub-basin and the boundary of the oceanic-continental crust. The first order vertical derivative appears in many speckled spots showing unstable perturbation of the calculation results (Figure 5c). The calculations of the second vertical derivative show that for the UTC method, the derivative value also appears a little unstable in some sub-regions of the southwest basin, such as along the spreading ridge axis in the northeast (Fig. 5b). However, this map has reflected quite well the structural elements in the study area, such as the spreading ridge axis, NE-SW, and sub-meridian fault systems. On the contrary, looking at the results of calculating the second derivative by the FFT method (Figure 5d), we see that the obtained results are fuzzy. The second derivative values fluctuate very strongly, forming unstable value regions, and the gravity field image does not reflect the structural elements in the study area.
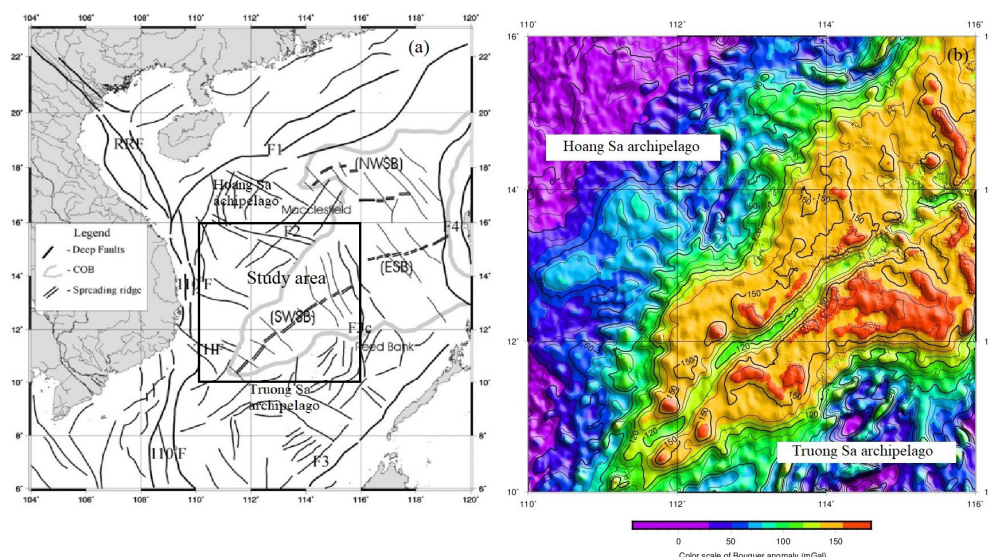

Figure 4. (a) Diagram of fault system [21] and location of the study area;
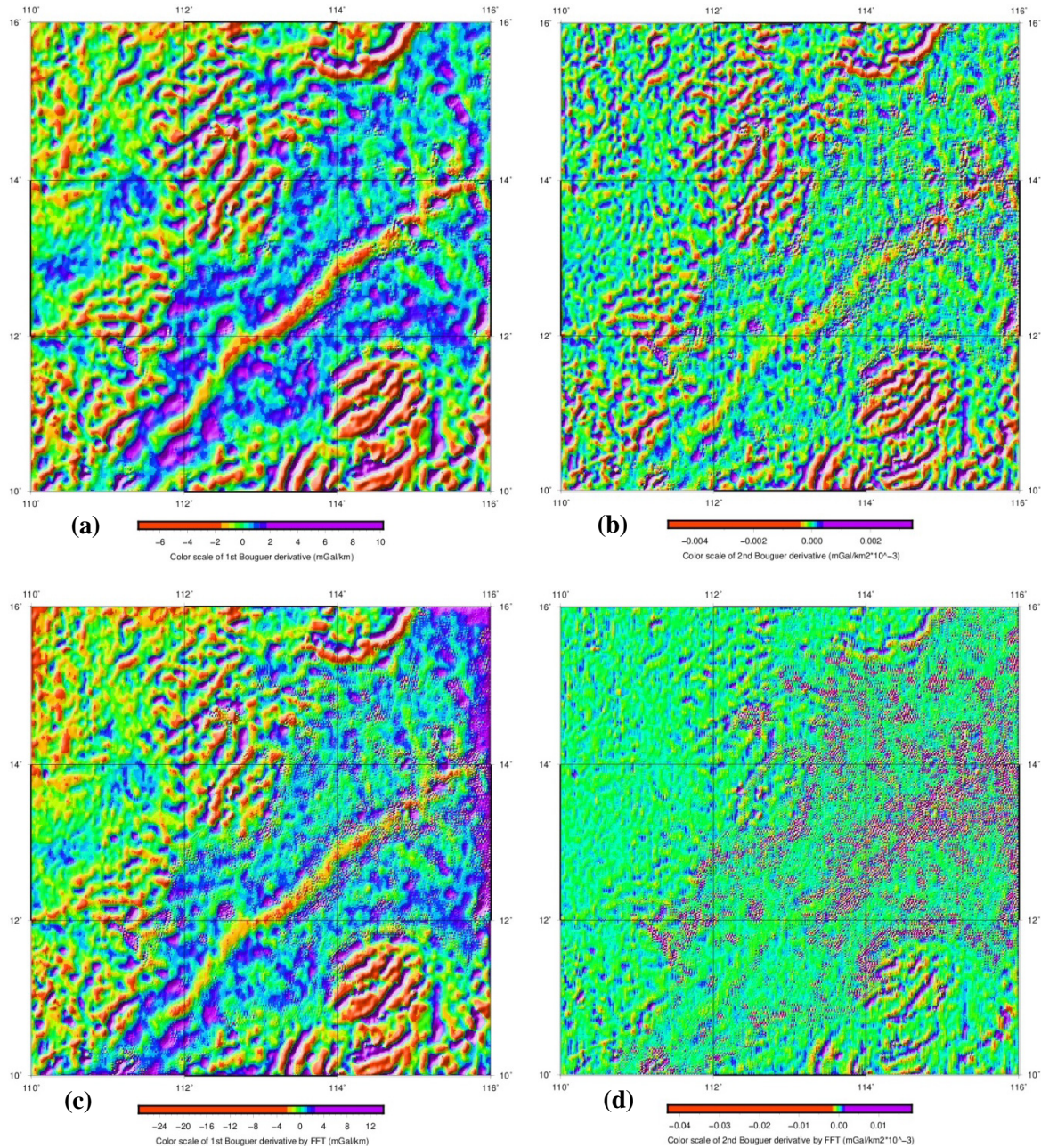(b) Bouguer gravity anomaly map of the study area

Figure 5. Vertical derivative maps of the Bouguer anomaly in the study area: the first (a) and second (b) order vertical derivatives are calculated by the UCT method, and the first (c) and second (d) derivatives are calculated by the FFT method

Some methods for determining the horizontal boundary of the field sources using vertical derivatives [1–4, 22–24] calculated by the FFT method will inevitably lead to instability in the calculation results. For example, below is the result of calculating the logistic function of the total horizontal gradient (LTHG) [3] using the vertical derivative of the entire horizontal gradient:

$$LTHG = \left[1 + exp\left(-\frac{\dfrac{\partial THG}{\partial z}}{\sqrt{\left(\dfrac{\partial THG}{\partial x}\right)^2 + \left(\dfrac{\partial THG}{\partial y}\right)^2}} \right) \right]^{-\alpha}$$

We see the LTHG formula that if we use the FFT method to calculate the vertical derivative, the result will be far different from the UTC method. Figure 6a is a map of LTHG calculated by the UTC method with very stable results, the sequence of peak points is obvious.

Meanwhile, the LTHG map calculated by the FFT method (Figure 6b) gives bad results in the Southwest sub-basin. It is clear that the accuracy of the vertical derivative has a significant influence on the quality of the LTHG map.
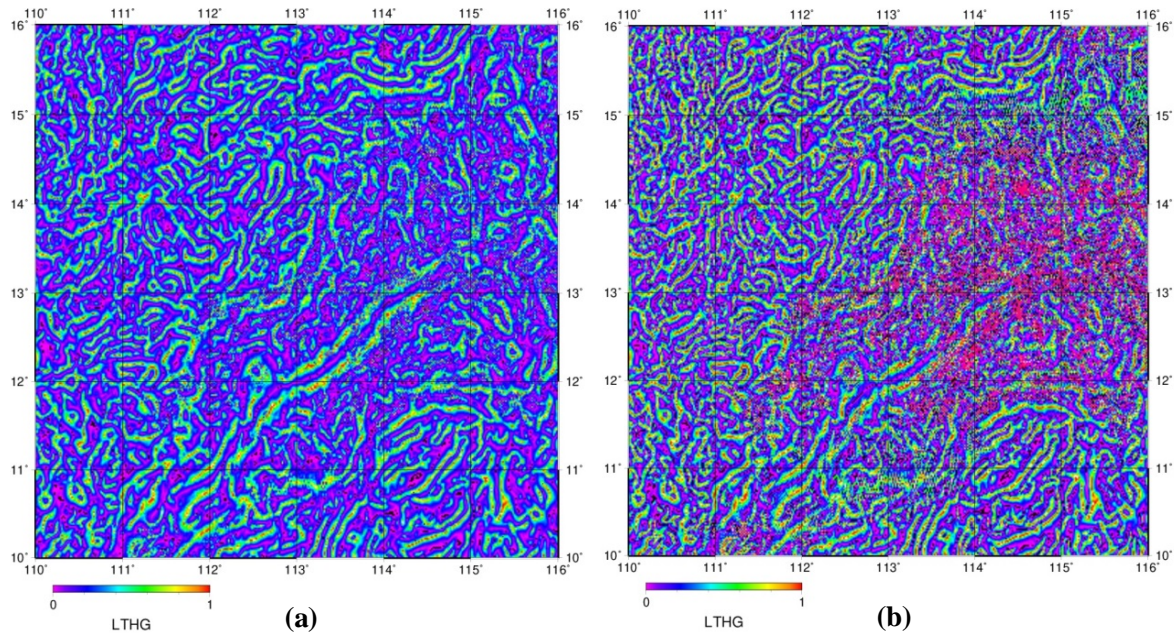

Figure 6. Comparison of results of calculating LTHG by UTC method (a) and by FFT method (b)

CONCLUTION

Equations (4), (5), and (6) allow for the calculation of the first, second, and third derivatives of potential field anomalies with higher stability and accuracy than the conventional methods, especially in case of the noisy data. Calculating the first and second order vertical derivatives of the gravity anomaly by the UTC method achieves high accuracy, making an important contribution to the processing and interpretation of gravity data using vertical derivative: the obtained results have high accuracy and stability easier to

determine the horizontal geological structure boundaries. The UTC method can be used to calculate the downward continuation over some deep water areas to increase the detail of local, shallow geological structures, thereby contributing to clarifying the image of geological structure in the study area.

Technology under grand number VAST06.01/21–22.

REFERENCES

[1] Miller, H. G., and Singh, V., 1994. Potential field tilt—a new concept for location of potential field sources. *Journal of applied Geophysics*, *32*(2-3), 213–217. https://doi.org/10.1016/0926-9851(94)90022-1

[2] Pham, L. T., Oksum, E., Do, T. D., and Huy, M. L., 2018. New method for edges detection of magnetic sources using logistic function. *Geofizicheskiy Zhurnal*, *40*(6), 127–135. https://doi.org/10.24028/gzh.0203-3100.v40i6.2018.151033

[3] Pham, L. T., Van Vu, T., Le Thi, S., and Trinh, P. T., 2020. Enhancement of potential field source boundaries using an improved logistic filter. *Pure and Applied Geophysics*, *177*(11), 5237–5249. https://doi.org/10.1007/s00024-020-02542-9

[4] Cooper, G. R. J., and Cowan, D. R., 2006. Enhancing potential field data using filters based on the local phase. *Computers & Geosciences*, *32*(10), 1585–1591. https://doi.org/10.1016/j.cageo.2006.02.016

[5] Nasuti, Y., Nasuti, A., and Moghadas, D., 2019. STDR: A novel approach for enhancing and edge detection of potential field data. *Pure and Applied Geophysics*, *176*(2), 827–841. https://doi.org/10.1007/s00024-018-2016-5

[6] Evjen, H. M., 1936. The place of the vertical gradient in gravitational interpretations. *Geophysics*, *1*(1), 127–136. https://doi.org/10.1190/1.1437067

[7] Peters, L. J., 1949. The direct approach to magnetic interpretation and its practical application. *Geophysics*, *14*(3), 290–320. https://doi.org/10.1190/1.1437537

[8] Trejo, C. A., 1954. A note on downward continuation of gravity. *Geophysics*, *19*(1), 71–75. doi: 10.1190/1.1437972

[9] Ackerman, J., 1971. Downward continuation using the measured vertical gradient. *Geophysics*, *36*(3), 609–612. https://doi.org/10.1190/1.1440196

[10] Zhang, H., Ravat, D., and Hu, X., 2013. An improved and stable downward continuation of potential field data: The truncated Taylor series iterative downward continuation methodImproved and stable downward continuation. *Geophysics*, *78*(5), J75–J86. https://doi.org/10.1190/geo2012-0463.1

[11] Abedi, M., Gholami, A., and Norouzi, G. H., 2013. A stable downward continuation of airborne magnetic data: A case study for mineral prospectivity mapping in Central Iran. *Computers & Geosciences*, *52*, 269–280. https://doi.org/10.1016/j.cageo.2012.11.006

[12] Tran, K. V., & Nguyen, T. N., 2020. A novel method for computing the vertical gradients of the potential field: application to downward continuation. *Geophysical Journal International*, *220*(2), 1316–1329. https://doi.org/10.1093/gji/ggz524

[13] Hu, M., Li, L., Jin, T., Jiang, W., Wen, H., and Li, J., 2021. A new $1' \times 1'$ global seafloor topography model predicted from satellite altimetric vertical gravity gradient anomaly and ship soundings BAT_VGG2021. *Remote Sensing*, *13*(17), 3515. https://doi.org/10.3390/rs13173515

[14] Nguyen, T. N., Van Kha, T., Van Nam, B., and Nguyen, H. T. T., 2020. Sedimentary basement structure of the Southwest Sub-basin of the East Vietnam Sea by 3D direct gravity inversion. *Marine Geophysical Research*, *41*(1), 1–12. doi: 10.1007/s11001-020-09406-w

[15] Hinojosa, J. H., and Mickus, K. L., 2002. Hilbert transform of gravity gradient profiles: Special cases of the general gravity-gradient tensor in the Fourier transform domain. *Geophysics*, *67*(3), 766–769. doi: 10.1190/1.1484519

[16] Ramadass, G., Arunkumar, I., Rao, S. M., Mohan, N. L., and Sundararajan, N., 1987. Auxiliary functions of the Hilbert transform in the study of gravity anomalies. *Proceedings of the Indian Academy of Sciences-Earth and Planetary Sciences*, *96*(3), 211–219. https://doi.org/10.1007/BF02841613

[17] Fedi, M., and Florio, G., 2002. A stable downward continuation by using the ISVD method. *Geophysical Journal International*, *151*(1), 146–156. doi: 10.1046/j.1365-246X.2002.01767.x

[18] Chen, T., and Yang, D., 2022. Gravity gradient tensors derived from radial component of gravity vector using Taylor series expansion. *Geophysical Journal International*, *228*(1), 412–431. https://doi.org/10.1093/gji/ggab318

[19] Liu, J., Liang, X., Ye, Z., Liu, Z., Lang, J., Wang, G., and Liu, L., 2020. Combining multi-source data to construct full tensor of regional airborne gravity gradient disturbance. *Chinese Journal of Geophysics*, *63*(8), 3131–3143. doi: 10.6038/cjg2020O0044

[20] Liu, J., 2022. Using gravity gradient component and their combination to interpret the geological structures in the eastern Tianshan Mountains. *Geophysical Journal International*, *228*(2), 982–998. https://doi.org/10.1093/gji/ggab373

[21] Nguyen, N. T., & Nguyen, T. T. H., 2013. Topography of the Moho and earth crust structure beneath the East Vietnam Sea from 3D inversion of gravity field data. *Acta Geophysica*, *61*(2), 357–384. doi: 10.2478/s11600-012-0078-9

[22] Cooper, G. R., 2014. Reducing the dependence of the analytic signal amplitude of aeromagnetic data on the source vector direction. *Geophysics*, *79*(4), J55–J60. https://doi.org/10.1190/geo2013-0319.1

[23] Ferreira, F. J., de Souza, J., de B. e S. Bongiolo, A., and de Castro, L. G., 2013. Enhancement of the total horizontal gradient of magnetic anomalies using the tilt angle. *Geophysics*, *78*(3), J33–J41. https://doi.org/10.1190/geo2011-0441.1

[24] Sumintadireja, P., Dahrin, D., and Grandis, H., 2018. A Note on the Use of the Second Vertical Derivative (SVD) of Gravity Data with Reference to Indonesian Cases. *Journal of Engineering & Technological Sciences*, *50*(1), 127–139.